INDERSCIENCE PUBLISHERS
Linking academia, business and industry through research

International Journal of Machining and Machinability of Materials

ISSN online: 1748-572X - ISSN print: 1748-5711
https://www.inderscience.com/ijmmm

Analyses of chip morphology and cutting force in the threading of austenitic stainless steel

Carlos Eduardo Costa, Milton Luiz Polli, Adriano Perpetuo de Lara

DOI: 10.1504/IJMMM.2024.10067460

Article History:

Received:	25 April 2024
Last revised:	17 July 2024
Accepted:	22 July 2024
Published online:	18 March 2025

Analyses of chip morphology and cutting force in the threading of austenitic stainless steel

Carlos Eduardo Costa, Milton Luiz Polli* and Adriano Perpetuo de Lara

PPGEM,
Department of Mechanics,
Federal University of Technology,
Paraná, Rua Deputado Heitor Alencar Furtado, 5000,
Ecoville, Curitiba, PR, CEP 81280-340, Brazil
Email: carlos.costa0121@gmail.com
Email: polli@utfpr.edu.br
Email: adriano_perpetuo@hotmail.com
*Corresponding author

Abstract: Chip formation and cutting force behaviour in the threading of austenitic stainless steels are important aspects that influence the performance of the process. The present paper analyses the impact of different infeed methods on the chip morphology and main cutting force in the threading of AISI 304L stainless steel. The results showed that long helical chips were predominant for the three infeed methods. The saw-tooth profile along the edges was present in the microscopic morphology of the chip, which is a characteristic of serrated chips. Flank and incremental infeed methods resulted in better chip generation and less restriction to chip flow when compared to the radial infeed. The main cutting force increased with the number of machined workpieces due to the progressive tool wear and the consequent changes in tool geometry. Radial infeed resulted in higher main cutting force than the other methods due to the V-shaped chip formation and higher stress concentration at the tool nose that accelerated tool wear.

Keywords: threading; stainless steel; infeed method; chip morphology; cutting force.

Reference to this paper should be made as follows: Costa, C.E., Polli, M.L. and de Lara, A.P. (2025) 'Analyses of chip morphology and cutting force in the threading of austenitic stainless steel', *Int. J. Machining and Machinability of Materials*, Vol. 27, No. 1, pp.70–84.

Biographical notes: Carlos Eduardo Costa obtained his PhD in Mechanical Engineering from the Federal University of Technology – Parana (UTFPR) – Brazil. He has experience in manufacturing processes, especially in turning, milling and threading.

Milton Luiz Polli is currently a Professor at the Federal University of Technology – Parana (UTFPR) in Curitiba, Brazil. He obtained his PhD in Mechanical Engineering from the Federal University of Santa Catarina – Brazil. He works in the optimisation of machining processes and works mainly on the following topics: drilling, turning, milling, grinding, high-speed machining, and regenerative vibrations.

Adriano Perpetuo de Lara holds a Master's degree in Mechanical Engineering from the Federal University of Technology – Parana (UTFPR) – Brazil. He has experience in Machining Processes and regenerative vibrations.

1 Introduction

Thread machining is particularly challenging due to the complexities associated with the formation and flow of the chips in the cutting zone. Given the distinctive characteristics inherent to these materials, this challenge becomes even more pronounced when working with austenitic stainless steels. They exhibit poor machinability because of their mechanical properties and tendency to work hardening (San-Juan et al., 2015), leading to rapid tool wear and deteriorated surface finishing. Thread machining encompasses a variety of methods, such as turning, tapping, milling, grinding, and rolling. Long-threaded surfaces can be machined by whirling (Botak et al., 2022). Turning and milling processes are distinguished by their superior machining efficiency and their capacity to adjust geometric parameters finely, ensuring the elimination of tool-thread interference (Xu et al., 2023). On the other hand, bolts with threads machined through the rolling process exhibit superior fatigue performance than those machined using the cutting process (Bartsch and Feldmann, 2021).

The behaviour of machining forces in threading diverges from that observed in the turning process. Kafkas (2010) reported that the specific cutting forces reduce at the beginning of the process and then increase with consecutive passes in threading. Khoshdarregi and Altintas (2015) proposed a model to predict the cutting forces in threading with multi-point inserts and different tooth profiles. They observed a notable disparity between simulation and experimental results, particularly during final passes, attributable to wider chips and more pronounced chip interference. Hajdu et al. (2023) introduced a curved uncut chip thickness model as part of a mechanistic approach to predict the cutting forces for general uncut chip geometries. The model's effectiveness for various cutting edge geometries including threading inserts was presented in case studies. They encountered challenges in experimentally validating their findings due to the extreme cutting conditions. Unmodelled phenomena, changes in friction coefficients, chip segmentation, and heat generation during chip formation may also affect the validation, which are hard to monitor and control. Onysko et al. (2023) developed an algorithm for calculating the thread profile depending on the value of the back rake parameter of the threading cutter tool. The possible divergence from the tool-join pitch diameter was based on the possible divergence from the tool-join pitch predicted. Khoei et al. (2023) investigated the tribological and wear performance of AlTiN-based coating systems at high temperatures when threading super duplex stainless steel. The investigation has been conducted into the energy needed to perform the cut and induce friction among the proposed AlTiN-based coating systems. They reported that the thread machining results validated the tribometer data, confirming that the tribometer can be used for analysing extreme friction conditions.

The directions that the cutting tool penetrates the workpiece in each pass during the threading are defined by the infeed method, which plays an important role in the process performance. In their recent study, Ghogha et al. (2024) analysed the effect of infeed strategies on the flank wear during thread milling of grey cast iron. They found that incremental and modified flank infeed methods resulted in significant improvements compared to the radial infeed method. Costa and Polli (2021) investigated the influence of the infeed method on tool life, surface microhardness, and the temperature during threading of AISI 304L stainless steel. By using the use incremental infeed it was possible to reduce temperature and surface hardening depth, as well as increase tool life. Nevertheless, the paper did not address important aspects like chip morphology and cutting forces. Understanding chip formation and cutting force behaviour in threading of austenitic stainless steels is essential to optimising the process. Moreover, the models to predict the cutting forces in this process still present significant limitations. Thus, additional experimental studies are required to draw firm conclusions about the topic. In this context, this paper analyses the impact of three distinct infeed methods on the chip morphology and main cutting force in the threading of AISI 304L stainless steel.

2 Theoretical chip cross-sectional area

The theoretical chip cross-sectional area (S_i) for each threading pass for the three infeed methods is represented in Figure 1.

In the first pass, as the depth of the cut (a_p) is smaller than the tool nose radius (r_ε), the contour of the chip cross-sectional area (S_1) appears as an arc segment and is similar for the three infeed methods. From the next threading pass, the chip cross-sectional area starts to be formed by different regions. In this case, as described by Akyildiz (2013) there is a region A delimited by an internal boundary generated by the tool nose radius at the previous pass and an external boundary generated by the tool nose radius at the current pass. There are also regions B and B′ whose internal boundaries are generated by the tool nose radius at the previous pass and linear external boundaries generated by the cutting edges. Moreover, there are regions C and C′ where the internal and external boundaries are linear and generated by the cutting edges during the previous and current passes, respectively.

The distribution of these regions differs between the infeed methods. In the radial method, the linear regions are symmetrically arranged, resulting in a V-shaped chip. In this case, the chip thickness at both sides of the thread chip corresponds to half of the chip thickness at its root. In the flank method, the linear region is concentrated on one side of the thread chip, and the chip shape is similar to that of a cylindrical turning operation. The linear region in the incremental method is similar to the one of the flank method, but it changes its position in every thread pass, alternating between both sides of the thread. The chip thickness at one side of the chip thread is closer to the chip thickness at its root.

Figure 1 Chip cross-sectional area for each pass (S_i) for different infeed methods (see online version for colours)

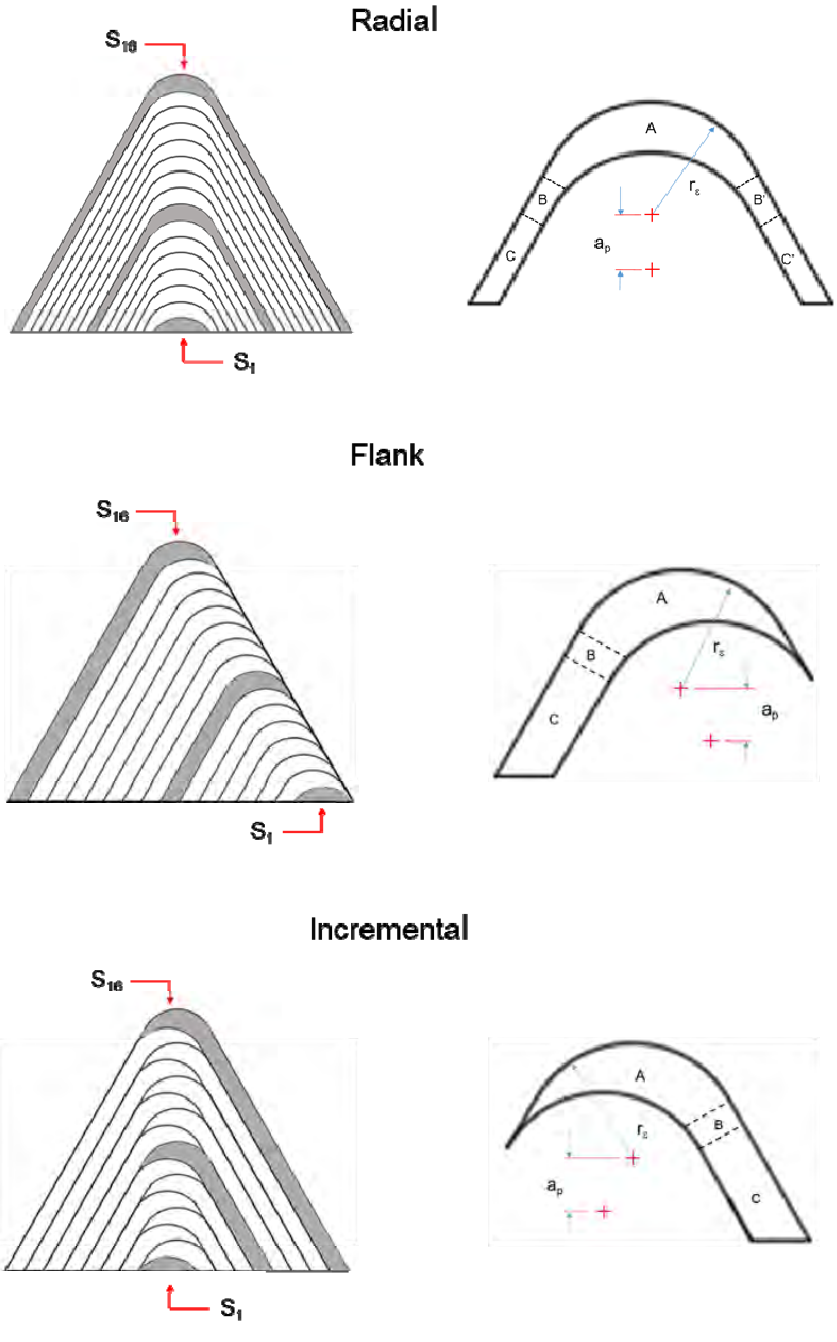

The chip thickness remains constant in the linear region regardless of the infeed method. In the radial infeed, the chip thickness changes throughout the nonlinear region. Meanwhile, for the flank and incremental methods, the chip thickness changes sharply

only in a reduced portion. Once machining forces have different behaviour in the nonlinear region of the chip, significant differences in force magnitudes are expected between the infeed methods.

3 Experimental procedure

The material under investigation in this study is the AISI 304L stainless steel, selected in a solution-annealed state, exhibiting a hardness of 218 HB. The material's tensile strength was determined to be 629 MPa, with an elongation of approximately 42%. The chemical composition of the steel is detailed in Table 1. The workpiece samples employed in the experiments had a diameter of 16 mm and a length of 200 mm, as illustrated in Figure 2. Specifically, the thread portion of the workpieces was 170 mm in length, featuring a pitch of 2.0 mm. The experimental procedures were conducted in a Nardini Diplomat CNC lathe.

Figure 2 Workpiece samples (see online version for colours)

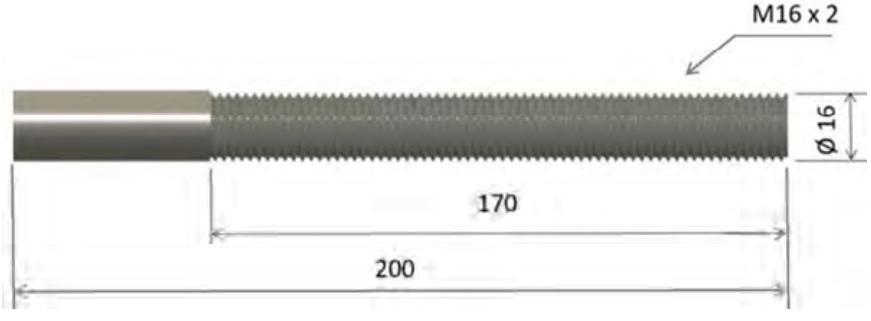

Table 1 Chemical composition of AISI 304L (%)

C	*Cr*	*Mn*	*Mo*	*N*	*Ni*	*P*	*S*	*Si*
0.024	18.25	1.570	0.500	0.085	8.040	0.037	0.028	0.280

The experiments utilised cemented carbide inserts, specifically the RG16VM01A002M 1125, which were coated with TiN for enhanced performance. Three distinct infeed methods – radial, flank and incremental – were applied during the tests. The cutting speed was set to 50 m/min, and the desired thread height of 1.227 mm was achieved through 16 passes with a constant depth of cut. No cutting fluids were used during the tests. Ring gauges were employed to check the conformity of the threaded samples.

The theoretical chip cross-sectional area (S_i) for each threading pass for the three infeed methods was modelled in a CAD software (Solidworks) based on the parameters used in the experiments to determine their values.

Chip morphology was evaluated using a Zeiss EVO MA15 scanning electron microscope (SEM). The main cutting force (F_c) during the turning thread trials was measured using a Kistler 9257B piezoelectric dynamometer attached to a Kistler 5070A charge amplifier, which in turn was connected to a National Instruments USB-6259B data acquisition unit and a microcomputer (Figure 3).

Figure 3 Schematic diagram of experimental setup (see online version for colours)

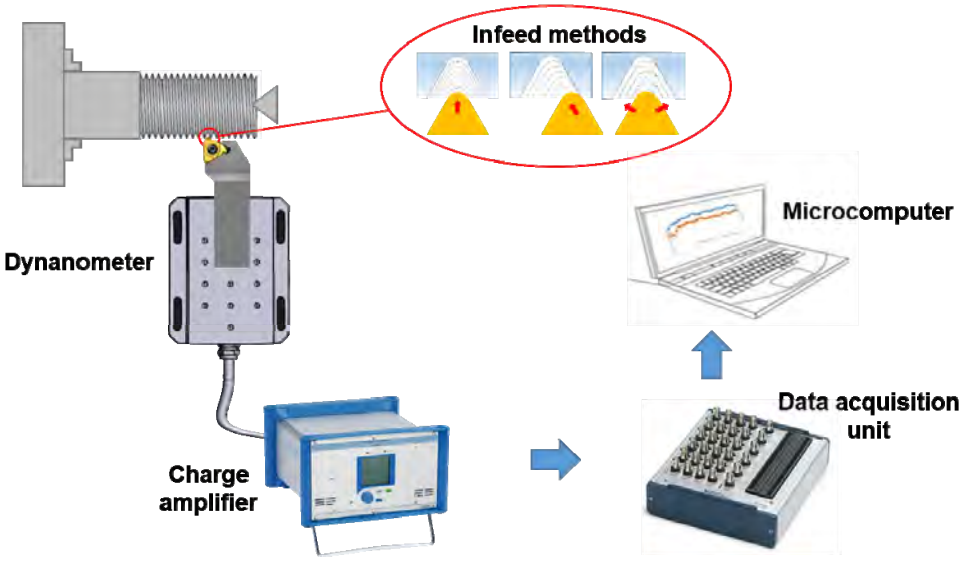

4 Results and discussions

Figure 4 illustrates the chip formation mechanism for threading 304L stainless steel. During the experiments of the present work, the saw-tooth profile along the edges was observed in the microscopic morphology of the chip for all the infeed methods. This is a characteristic of serrated chips. Depending on the operation and cutting conditions, the chip formed when machining 304L stainless steel may be continuous or serrated. The result is associated with material deformation in the primary zone, contact between the chip and tool in the secondary zone, and temperature rise due to deformation in both cutting zones. According to Wang and Liu (2014), in continuous chip formation, shear constantly occurs, while serrated chip formation involves the combined effect of ductile mode failure and adiabatic shear. In the formation of the serrated chips, small lamellae occur instead of shear bands, as shown in Figure 4.

Images of the free surface of the chip obtained during the last pass of the first and seventh threaded workpieces using the radial infeed are presented in Figure 5. The central region of the V-shaped chip is associated with the formation of the thread root, resulting from the contact between the tool nose radius (r_ε = 0.2 mm) and the workpiece material. Whilst the thread flanks are generated by the cutting edges. The chip surface presents regions with different lamella structure orientations, which may be approximately parallel to the cutting edges or the tool nose. The chip deformation is higher at the central region of the chip than at its sides, resulting in distortions in the actual V-shaped chip. This condition is especially noticeable in the chip of the seventh workpiece owing to the higher tool wear. In this case, the tool was close to the end of its life and far from its initial geometry, resulting in higher chip deformation.

Figure 4 Chip formation in threading of 304L stainless steel (see online version for colours)

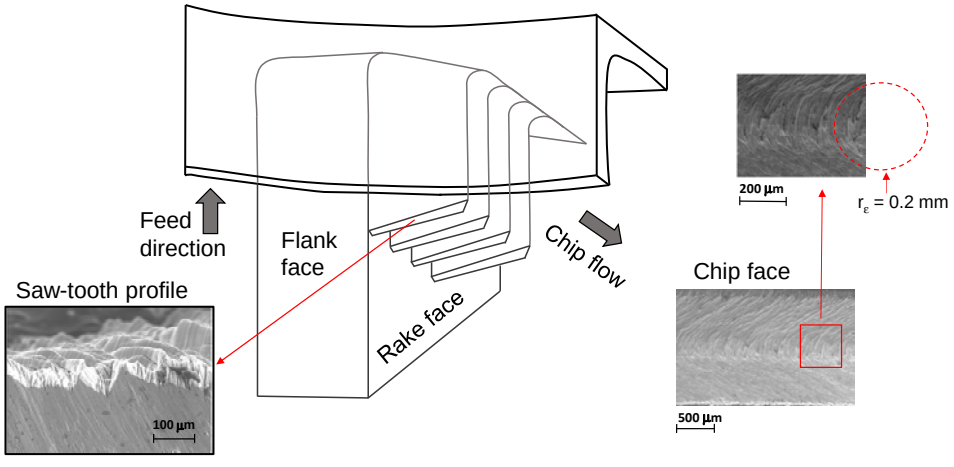

Figure 5 Chip obtained by using the radial infeed, (a) first workpiece (b) seventh workpiece (see online version for colours)

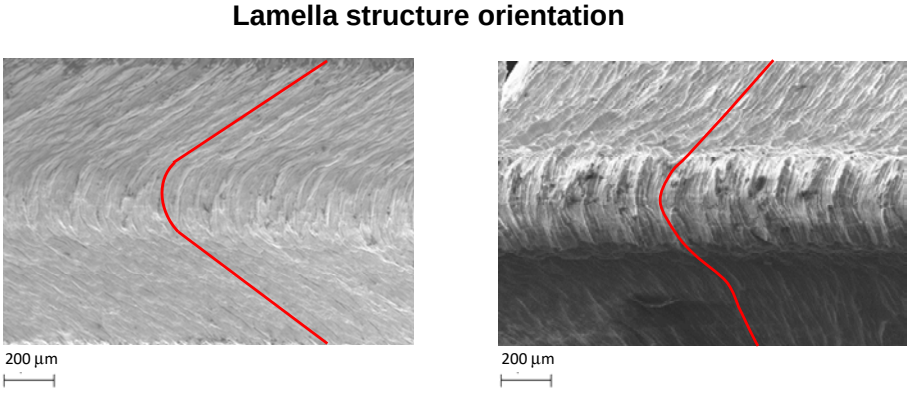

(a) (b)

Figure 6 illustrates images of the chips obtained during the last pass of the seventh threaded workpiece by the flank infeed and incremental infeed. Similar chips were found for both methods. These infeed methods resulted in better chip generation and less restriction to chip flow when compared to the radial infeed. The free surface presents two regions with different lamella structure orientations. In the major one, the orientation is parallel to the main cutting edge. In the corner one, the orientation is parallel to the tool nose. Chip deformation is considerably lower than radial infeed. The back surface of the chip that contacts the tool rake surface is smooth, while the free surface has more irregularities with the formation of a serrated profile. According to Zhang and Guo (2009), in all cutting operations, the plastic deformation of the back surface of the chip is constrained by the tool rake face, resulting in high contact pressure and frictional force when the chip slides over the tool rake face. These combined actions with high temperatures make the back surface of the chip shiny and smooth.

Figure 6 Chip surfaces, (a) incremental infeed (b) flank infeed (see online version for colours)

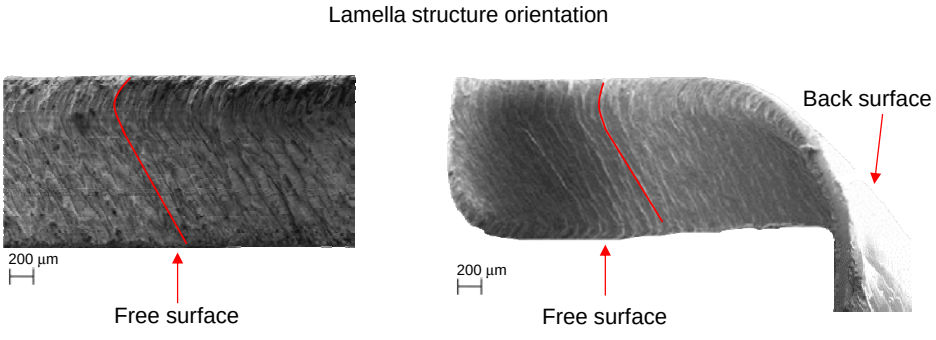

The long helical chip was predominant for the three infeed methods during the experiments. The helix's external side corresponded to the back surface of the chip, which presented a smoother appearance. In contrast, the inner side of the helix exhibited a rough surface and corresponded to the free surface of the chip.

The theoretical chip cross-sectional area found for each threading pass according to the parameters of the experiments is shown in Figure 7.

Figure 7 Chip cross-sectional area as a function of the number of passes (see online version for colours)

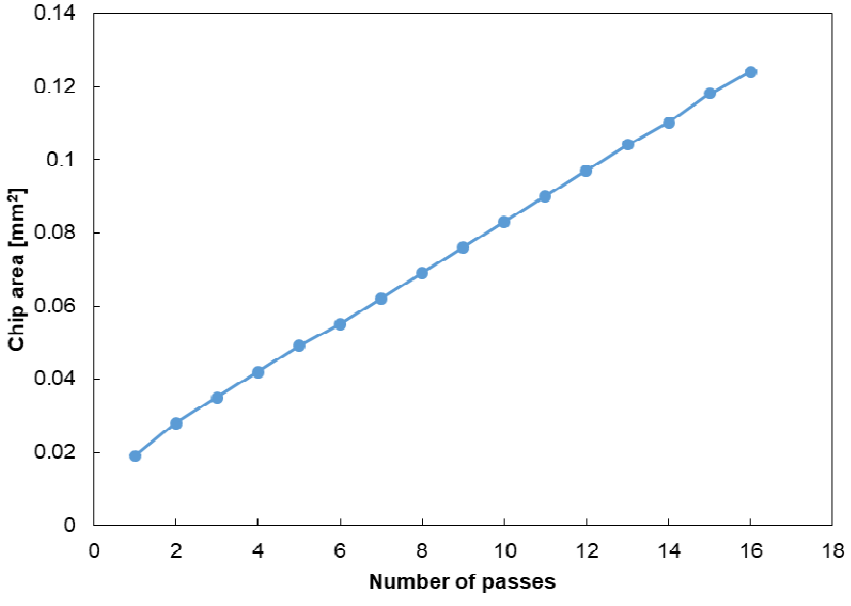

The chip cross-sectional area values are the same regardless of the infeed method. The chip cross-sectional area increases linearly with the increase in the number of passes, and the chip cross-sectional area of the last pass corresponds to approximately six times the chip cross-sectional area of the first one.

Figure 8 shows the evolution of the mean main cutting force according to the threading passes for the first machined workpiece, where the error bars correspond to two standard deviations calculated from three measurements. The main cutting force increases with the number of threading passes. This is mainly because the chip area increases as the successive threading passes are performed with a constant depth of cut. Although the chip cross-sectional area values are the same for the different infeed methods, higher main cutting forces were observed for the radial infeed compared to the flank and incremental infeed. As the number of threading passes increases, the interference between the chips on the tool rake face becomes evident for the radial infeed. According to Kafkas (2010), each cutting edge produces chips simultaneously during thread machining. Chips travel in different directions, colliding with each other and interfering with subsequent cuts, which affect the forces acting in the shear area or on the tool rake face. Moreover, the distribution of regions with different chip sections also influences the behaviour of the cutting force. For the radial infeed, in the linear regions where the cut is performed by the cutting edges, the chip is constrained on one side and free on the other. Meanwhile, in the region where the tool nose radius performs the cut, the chip is constrained on both sides by the linear regions. According to Akyildiz (2013), this results in high compressive stress during the process due to the differences in the chip thickness ratio in these regions.

Figure 8 Main cutting force as a function of the number of passes for the first workpiece (see online version for colours)

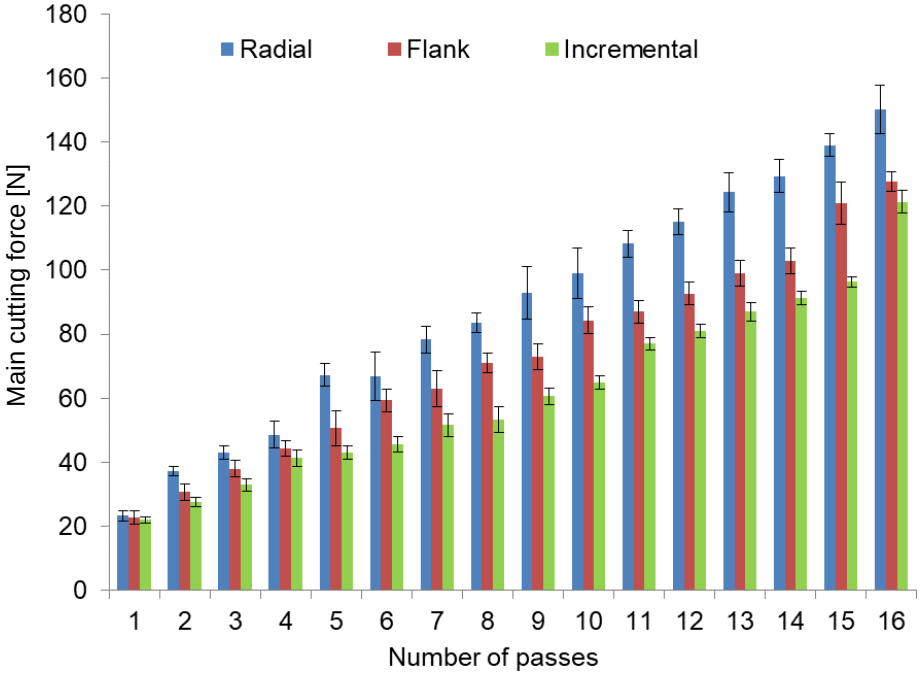

As the successive threading passes are performed, the cutting conditions become more severe, and more energy is needed to deform the chip, increasing the main cutting force. The work-hardening tendency of the austenitic stainless steel during the machining process may also contribute to the increase in the main cutting force for all the infeed methods.

The maximum values of the main cutting force obtained during the machining of each workpiece for the different infeed methods are shown in Figure 9.

Figure 9 Maximum values of the main cutting force as a function of the number of threaded workpieces (see online version for colours)

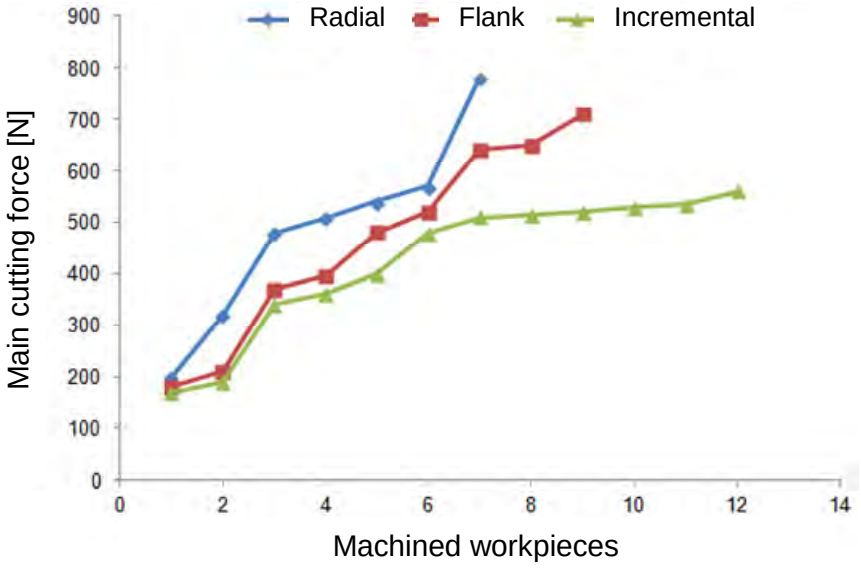

There was a small difference in values for the three infeed methods for the first workpiece. However, the maximum main cutting force values increased with the number of machined workpieces due to the progressive tool wear and the consequent changes in tool geometry. Radial infeed resulted in higher main cutting force than the other methods due to the V-shaped chip formation and higher stress concentration at the tool nose that accelerated tool wear. There was a uniform growth up to 540 N associated with the sixth workpiece, followed by a sharp rise for the final approved workpiece, achieving a value of 780 N. As mentioned before, high chip deformation was observed for this condition. The flank infeed exhibited main cutting force values that fell between those of radial and incremental infeeds. The main cutting force increased almost linearly up to the last approved workpiece, where a value of 710 N was reached. Incremental infeed provided lower main cutting forces during the process due to lower tool wear. This method uses both cutting edges and changes the thread flanks and sides of the tool in every pass. The main cutting force curve behaviour for this method was similar to the flank infeed until the sixth workpiece, after which it displayed a more gradual rise until reaching the final approved workpiece, where it peaked at a maximum force of 560 N.

The behaviour of the main cutting force during the final pass in machining the last approved workpiece for each infeed method is illustrated in Figure 10. In radial infeed machining, the main cutting force increased steadily over time due to the tool's rapid

wear progression resulting in higher chip deformation [Figure 5(b)]. Flank infeed resulted in some fluctuation in the main cutting force, likely attributed to contact between the minor cutting edge and the opposite thread flank, as well as the tendency of the stainless steel to adhere to the tool. The main cutting force was more stable during the machining with the incremental infeed than the other methods. These findings are associated with the varying progression of the tool wear among the three infeed methods, which consequently influenced the surface quality and accuracy of the thread profile.

Figure 10 Main cutting force during the final pass in machining the last approved workpieces (see online version for colours)

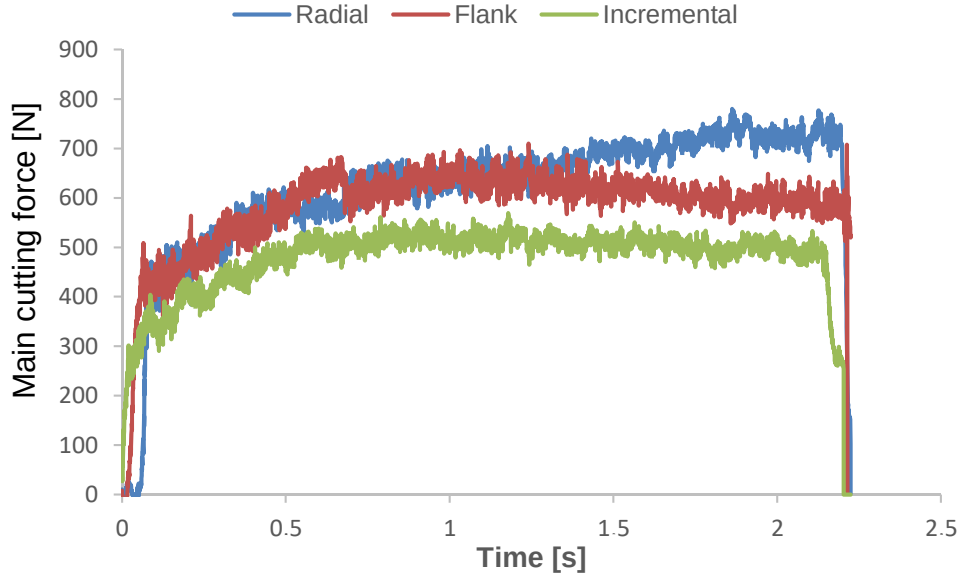

Figure 11 Last approved threaded workpieces produced with (a) radial infeed, (b) flank infeed and (c) incremental infeed (see online version for colours)

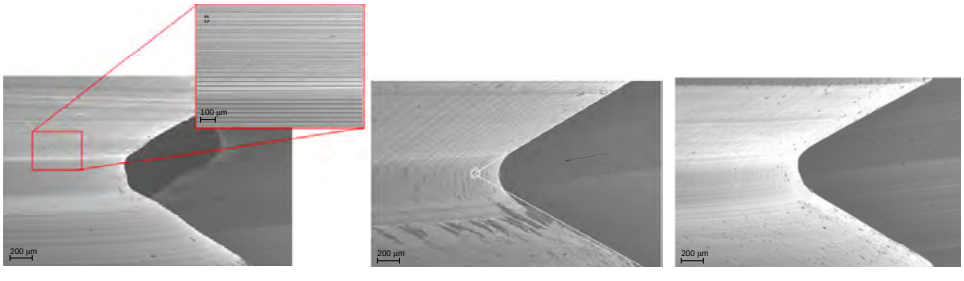

(a) (b) (c)

Images of the last approved threaded workpieces produced with each infeed method are presented in Figure 11. Radial streaks can be observed on the surface of the thread flank of the seventh workpiece using the radial infeed [Figure 11(a)]. These streaks exhibit greater spacing and depth from the thread's root to the flank. They are caused by tool microchipping, material adhesion on the tool cutting edge, and loose particles between

the workpiece and the tool. In the thread root, the influence of tool tip wear is evident. The thread root is formed by the tool tip geometry during the final pass.

Figure 12 illustrates the profile of the resulting thread on the seventh workpiece, as well as the condition of the tool after machining this workpiece with radial infeed. Excess material can be seen on the thread flank and root that was not removed due to wear on the flank and tip of the tool. The error Δ_w in the thread flank profile is influenced by the tool wear and, as indicated by Koleva et al. (2017), can be calculated based on flank wear *VB* and clearance angle (α), as shown in equation (1). However, in addition to flank wear, tool tip wear and microchipping on the cutting edges also have a significant impact on the profile of the machined thread.

$$\Delta_w = VB \tan \alpha \tag{1}$$

Despite the observed deviation from the original tool tip geometry, this workpiece was still approved during gauge inspection.

Figure 12 (a) Thread profile of the seventh workpiece machined with radial infeed (b) Tool after machining this workpiece (see online version for colours)

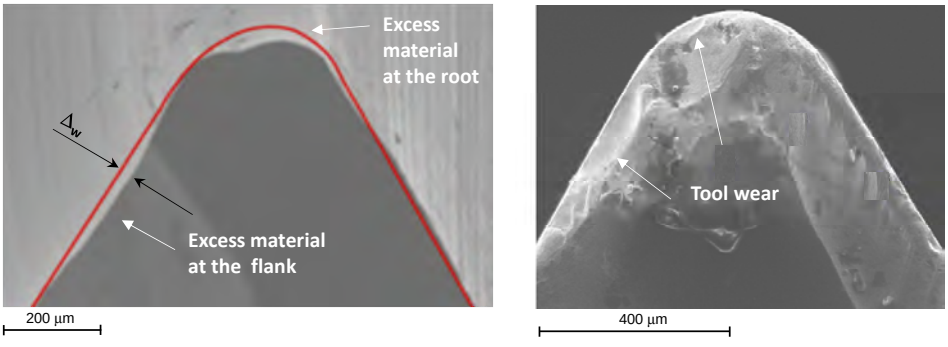

(a) (b)

An example of a thread obtained using the flank infeed, from the ninth workpiece is presented in Figure 11(b). The best surface finish is observed on the flank of the thread generated by the main cutting edge. Significant surface deterioration near the thread's root was observed on the flank generated by the minor cutting edge due to material adherence.

A uniform surface appearance is observed on both thread flanks of the twelfth workpiece obtained using the incremental infeed [Figure 11(c)], characteristic of the alternating cutting method employed. Good quality is also observed at the root of the thread. Figure 13 shows an overlay of images depicting the thread profile and the tool used for machining this workpiece. It can be observed that the profile of the worn tool is mirrored in the resulting machined thread. During the machining process, as the tool gradually wears, its original profile changes. Consequently, these alterations have direct impact on the accuracy of the machined thread, potentially deviating from the intended specifications.

Figure 13 Tool condition and thread profile of the twelfth workpiece machined with incremental infeed (see online version for colours)

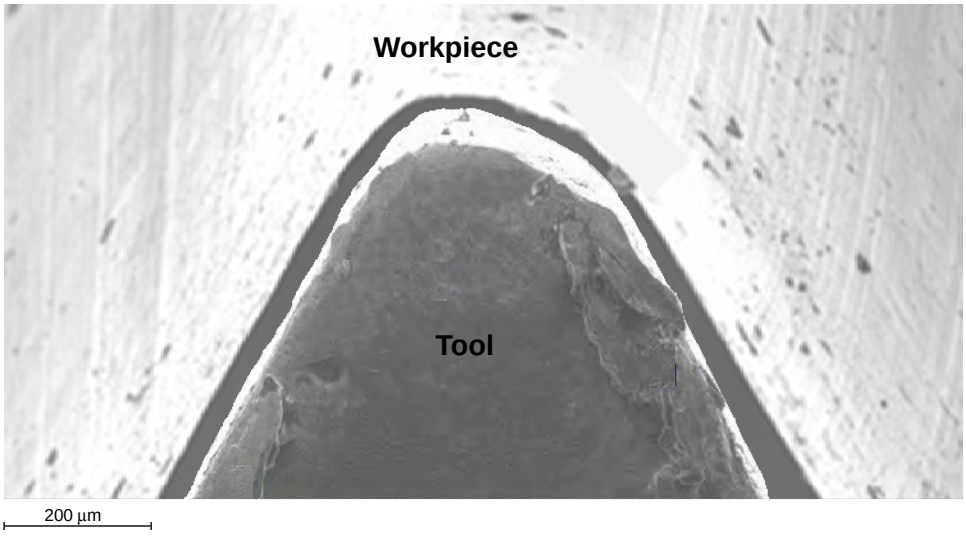

Table 2 summarises the findings from the experiments conducted, focusing on three key aspects across different infeed methods. These aspects include chip morphology, the count of approved workpieces, and the maximum main cutting force observed during machining the last approved workpieces.

Table 2 Experimental results summary

Infeed method	*Chip morphology*	*Approved workpieces*	*Maximum main cutting force for the last workpiece*
Radial	Long helical serrated V-shaped chips with higher deformation at the central region	7	780 N
Flank	Long helical serrated chips with major lamellae orientation parallel to the main cutting edge	9	710 N
Incremental	Long helical serrated chips with major lamellae orientation parallel to the main cutting edge	12	560 N

5 Conclusions

This paper explores the impact of different infeed methods on chip morphology and main cutting force during the threading process of AISI 304L stainless steel. From the results, the following conclusion can be drawn:

- Long helical chip was predominant for the three infeed methods. A saw-tooth profile along the edges was present in the microscopic morphology of the chip, which is a characteristic of serrated chips.

- The free surface of the chip obtained by the radial infeed presented a central region with lamella structure orientations parallel to the tool nose and side regions with lamella structure orientations parallel to the cutting edges. Flank and incremental infeed methods resulted in better chip generation and less restriction to chip flow when compared to the radial infeed. The free surface of the chip presented two regions with different lamella structure orientations. In the major one, the orientation was parallel to the main cutting edge, and in the corner one, the orientation was parallel to the tool nose.
- The main cutting force increases with the number of threading passes. This is mainly because the chip area increases as successive threading passes are performed. Moreover, the work-hardening tendency of the austenitic stainless steel during the machining process also contributes to the increase in the main cutting force. The main cutting forces measured for the flank and incremental methods were lower than those obtained for the radial infeed.
- The maximum main cutting force values increased with the number of machined workpieces due to the progressive tool wear and the consequent changes in tool geometry, which consequently influenced the surface quality and accuracy of the thread profiles. The radial infeed yielded a higher maximum main cutting force compared to the other methods due to the V-shaped chip formation and higher stress concentration at the tool nose that accelerated tool wear. The flank infeed exhibited main cutting force values that fell between those of radial and incremental infeeds. The incremental infeed provided lower main cutting forces during the threading process due to reduced tool wear.

Acknowledgements

Multi-User Center for Materials Characterization – CMCM of UTFPR-CT.

References

Akyildiz, H.K. (2013) ‘Evaluating of cutting forces in thread machining’, *International Journal of Advanced Manufacturing Technology*, Vol. 68, Nos. 5–8, pp.1601–1612, https://doi.org/10.1007/s00170-013-4957-2.

Bartsch, H. and Feldmann, M. (2021) ‘Reassessment of fatigue detail categories of bolts and rods according to EC 3-1-9’, *Journal of Constructional Steel Research*, Vol. 180, pp.106–588, https://doi.org/10.1016/j.jcsr.2021.106588.

Botak, Z., Pisačić, K., Horvat, M. and Ficko, M. (2022) ‘Manufacture of soybean extruder screws using a lathe with a whirling attachment’, *International Journal of Machining and Machinability of Materials*, Vol. 24, p.5, https://doi.org/10.1504/IJMMM.2022.126595.

Costa, C.E. and Polli, M.L. (2021) ‘Effects of the infeed method on thread turning of AISI 304L stainless steel’, *Journal of the Brazilian Society of Mechanical Sciences and Engineering*, Vol. 43, No. 253, https://doi.org/10.1007/s40430-021-02978-7.

Ghogha, H., Farahnakian, M. and Elhami, S. (2024) ‘Experimental and numerical studies on the flank wear during the thread milling; effect of infeed strategies in different cutting speeds’, *Tribology International*, https://doi.org/10.1016/j.triboint.2024.109899.

Hajdu, D., Astarloa, A., Kovacs, I. and Dombovari, Z. (2023) 'The curved uncut chip thickness model: a general geometric model for mechanistic cutting force predictions', *International Journal of Machine Tools and Manufacture*, Vol. 188, https://doi.org/10.1016/j.ijmachtools.2023.104019.

Kafkas, F. (2010) 'An experimental study on cutting forces in the threading and the side cut turning with coated and uncoated grades', *Journal of Manufacturing Science & Engineering*, Vol. 132, No. 4, p.041012, https://doi.org/10.1115/1.4001867.

Khoei, A.A., He, Q, De Paiva, J.M., Bipasha Bose, B. and Veldhuis, S.C. (2023) 'Assessment of the tribological and wear performance of new duplex AlTiN-based coating systems at high temperatures when threading super duplex stainless steel', *Journal of Manufacturing Processes*, Vol. 98, pp.285–301, https://doi.org/10.1016/j.jmapro.2023.05.042.

Khoshdarregi, M.R. and Altintas, Y. (2015) 'Generalized modeling of chip geometry and cutting forces in multi-point thread turning', *International Journal of Machine Tools and Manufacture*, Vol. 98, pp.21–32, https://doi.org/10.1016/j.ijmachtools.2015.08.005.

Koleva, S., Enchev, M. and Szecsi, T. (2017) 'Compensation of the deviations caused by mechanical deformations during machining of threads', *Procedia Manufacturing*, Vol. 13, pp.480–486, https://doi.org/10.1016/j.promfg.2017.09.066.

Onysko, O., Panchuk, V., Kopei, V., Pituley, L. and Lukan, T. (2023) 'Influence of back rake angle of a threading cutter on the drill-string tool-joint pitch diameter', *Lecture Notes in Mechanical Engineering*, pp.200–210, https://doi.org/10.1007/978-3-031-16651-8_19.

San-Juan, M., Martína, Ó., Tiedra, M.P., Santos, F.J., López, R. and Cebrián, J.A. (2015) 'Study of cutting forces and temperatures in milling of AISI 316L', *Procedia Engineering*, Vol. 132, pp.500–506, https://doi.org/10.1016/j.proeng.2015.12.525.

Wang, B. and Liu, Z. (2014) 'Serrated chip formation mechanism based on mixed mode of ductile fracture and adiabatic shear', *Proceedings of the Institution of Mechanical Engineers, Part B: Journal of Engineering Manufacture*, Vol. 228, No. 2, pp.181–190, https://doi.org/10.1177/0954405413497941.

Xu, H., Wei, P., Du, X., Hu, R., Liu, H., Kang, X. and Zhu, C. (2023) A study of precision grinding of micro-pitch internal thread for planetary roller screw mechanism', *Journal of Manufacturing Processes*, Vol. 106, pp.35–50, https://doi.org/10.1016/j.jmapro.2023.09.070.

Zhang, S. and Guo, Y.B. (2009) 'An experimental and analytical analysis on chip morphology, phase transformation, oxidation, and their relationships in finish hard milling', *International Journal of Machine Tools and Manufacture*, Vol. 49, No. 11, pp.805–813, https://doi.org/10.1016/j.ijmachtools.2009.06.006.